Structural Engineering and Mechanics, Vol. 11, No. 1 (2001) 17-34
DOI: http://dx.doi.org/10.12989/sem.2001.11.1.017

A variable layering system for nonlinear analysis of reinforced concrete plane frames

Ahmed B. Shuraim†

Civil Engineering Department, College of Engineering, King Saud University, P.O. Box 800, Riyadh 11421, Saudi Arabia

Abstract. An improved method has been developed for the computation of the section forces and stiffness in nonlinear finite element analysis of RC plane frames. The need for a new approach arises because the conventional technique may have a questionable level of efficiency if a large number of layers is specified and a questionable level of accuracy if a smaller number is used. The proposed technique is based on automatically dividing the section into zones of similar state of stress and tangent modulus and then numerically integrating within each zone to evaluate the sectional stiffness parameters and forces. In the new system, the size, number and location of the layers vary with the state of the strains in the cross section. The proposed method shows a significant improvement in time requirement and accuracy in comparison with the conventional layered approach. The computer program based on the new technique has been used successfully to predict the experimental load-deflection response of a RC frame and good agreement with test and other numerical results have been obtained.

Key words: computation; computer analysis; concrete structures; finite element analysis; layered systems; nonlinear analysis; nonlinear response; efficiency.

1. Introduction

Significant advances have been made during the past few decades in methods of nonlinear analysis for structures of varied forms and constituent materials. The advent and continuous development of finite element methods have allowed several aspects of reinforced concrete behavior to be modeled to various levels of accuracy and detail. In conjunction with these developments, the need for efficient algorithms that maintain a balance between accuracy and speed cannot be overemphasized. Examining the formulation and solution of a typical nonlinear finite element analysis of reinforced concrete structures indicates that in order to improve overall performance, the operations conducted at the section level, such as the computation of forces and rigidity parameters, must be improved.

One of the most widely used methods for computing stiffness parameters and forces over a cross section is the conventional layered approach. Despite its wide use, the efficiency of the conventional layered technique is questionable. It can be time consuming when excessive number of layers is used; it may cause numerical difficulty if the number of layers is not sufficient. Researchers have been using a number of layers in their analysis but it seems that no consensus on what constitute an optimum number of layers since the number may depends on a few variables including reinforcement

† Assistant Professor

ratio and strain variations. Because of the time required in analysis, researchers (Bazant *et al.* 1987, Kim *et al.* 1992, Kim *et al*. 1993, and Izzuddin *et al.* 1994) questioned its efficiency for nonlinear analysis of a wide range of structures. Many attempts have been made to improve or replace the layered approach; for example, Kim *et al.* (1992) selected the modified stiffness approach over the layered approach in their study of RC beams with softening. The success of the modified stiffness was described as limited; it gives high-speed results, although with limited accuracy, and at times, incorrect results. Consequently, a combined layered and nonlayered (modified stiffness) method was used over parts of the cross section (Kim *et al.* 1993). Another attempt to replace the layered approach was the introduction of an adaptive technique (Izzuddin *et al.* 1994). This technique presumed that the layered approach was necessary only in those zones of the structure that develop material inelasticity, while the elastic parts of the structure could be modeled using a less computationally intensive approach. Moreover, numerical integration over an entire cross section was utilized as an alternative approach. The latter approach was used by a number of researchers; for example, Marzouk *et al.* (1993) used a nine-point Simpson-type integration over slab thickness.

This study has a twofold task: first, it investigated the effect of the layering number on computation accuracy and time requirement; secondly, it proposed a variable layering technique that reduces the required time for computation while maintaining accuracy in the solution. Appropriate computer programs were written to carry out the objectives in general and to determine the applicability and suitability of the proposed technique.

To fulfil the objectives of this investigation, two sets of computer programs were written in this study: the first of which was capable of analyzing RC plane-framed structures while the other was geared to analyzing RC cross sections. The first set comprised two programs; the first of which was FRAME-CL that was based on the conventional layered approach while the other was FRAME-IL which was based on the proposed variable layering technique. They give internal forces and deformations under monotonic static loading with considerations of material and geometric nonlinearities. The second set was composed of two computer programs: SECTION-CL, based on the conventional layered approach; and SECTION-IL, based on the proposed variable layering technique. They give the axial load moment-curvature relationship for any assumed strain variation.

The purpose of using two sets of computer programs in this investigation was to allow more in-depth analysis of the features of the two approaches. SECTION programs have a relatively simplified algorithm and thus show force computation accuracy as affected by the number of layers representing the cross section. Such a simplified algorithm was intended to eliminate other sources of error that may occur in complex programs. FRAME programs have been used to test the two approaches for speed and accuracy under practical situations. Furthermore, FRAME-IL has been verified by comparing its prediction capability with test results and other analytical studies obtained from the technical literature.

1.1. General assumptions

1. Frames are subjected to static plane loading applied monotonically;
2. Materials have nonlinear elastic behavior with concrete post cracking modeled by a descending curve;
3. Perfect bond exists between concrete and steel;
4. Shear deformation is neglected, and so is the contribution of the web reinforcement.

1.2. Formulation of the beam-column element

The basic finite element for studying reinforced concrete plane frames is a two-node beam-column element having three degrees of freedom at each node. The cubic transverse displacement field, *v*, and the linear longitudinal displacement field, *u*, have been assumed for the deformed beam-column element. Axial strain is related to the displacement field by the following expression (Martin 1965):

$$\varepsilon(x, y) = u' + yv'' + 1/2(v')^2 \tag{1}$$

Where ($'$ and $''$) are the first and second derivatives with respect to *x*, respectively. *x* is the local coordinate passing from the face of the element through the centroid of the uncracked transformed section and *y* is the local perpendicular Cartesian coordinate following the right hand rule. The first two terms in Eq. (1) represent the linear effect, while the third term represents the nonlinear effect. The principle of virtual work is used to derive the incremental equilibrium equations that yield the element's tangent stiffness matrix in relation to the displacement vector as well as the force vector with respect to the local axes.

The tangent stiffness matrix is composed of geometric stiffness and material tangent stiffness where the latter is evaluated by the following expression (Shuraim 1997):

$$[k_m] = \int_{x=0}^{x=l} \int_A \{B_s\}^T E_t \{B_s\} dA dx \tag{2}$$

In Eq. (2), $\{B_s\}$ is the linear part of the strain-displacement vector resulting from the first two terms of Eq. (1). E_t is the tangent modulus of concrete or steel over the volume of the element. It is a function of strain, and since strain varies throughout the element, so does the tangent modulus. In the longitudinal direction of the element of length *l* (*x*-direction), integration is performed using three-point Gaussian quadrature. At every point, three quantities have to be evaluated over the cross-section of the element that has an area *A*. They are:

$$\int_A E_t dA$$

$$\int_A E_t y dA$$

$$\int_A E_t y^2 dA \tag{3}$$

where *y* is the *y* local coordinate measured from the reference line located at the centroid of the uncracked transformed section and is assumed to remain constant throughout the analysis.

Similarly, the internal force vector is evaluated by numerically integrating the following expression:

$$\{r\} = \int_{x=0}^{x=l} \int_A \{B\}^T \sigma dA dx \tag{4}$$

where $\{B\}$ is the strain-displacement matrix containing both the linear terms $\{B_s\}$, mentioned above, and the nonlinear terms $\{B_l\}$, resulting from the third term in Eq. (1); σ is the normal stress over the section; and the integration is to be performed over the volume of the element.

2. Conventional layered system

Generally, in the layered approach, the section is implicitly discretized into a number of concrete and steel layers in order to evaluate the quantities in Eqs. (3) and (4). For a plane frame element, it is usually assumed that each layer is in a state of uniaxial stress. The strain at the mid-height of each layer is used to represent the layers strain, which is used to compute the stress and tangent modulus based on the materials constitutive laws.

More than three decades ago, the layered concept was utilized (Bresler *et al.* 1964) for analyzing the time-dependent behavior of reinforced concrete structures. Later, a full formulation was given (Selna 1969) using the layered approach and linear analysis of materials. In the last three decades, the approach has been used by many researchers, though only a few brief examples are mentioned here. The approach has also been used for prestressed concrete frames (Kang *et al.* 1980) with the varied material properties within a frame element represented by a composite concrete and steel layer system. Similarly, the same approach has been used for the nonlinear analysis of RC frames (Sun and Gilbert 1993) as was previously used for RC slabs (Gilbert 1979). Moreover, computational models based on layered Mindlin plate finite element have been developed for the study of stiffened and cellular slabs (Abdel Rahman *et al.* 1986). Recently, the layered approach (Shuraim 1997) was applied to reinforced concrete frames following a similar formulation as that applied to prestressed concrete columns (Shuraim 1990). A similar layered-element formulation has also been used for integration through shell element thickness (Polak *et al.* 1993).

The current section presents a discussion of the treatment of the layered approach to Eq. (3) and Eq. (4). The three terms in Eq. (3) are assumed constant over a load increment. The computations of *EA*, *EM* and *EI* are achieved by integrating material tangent moduli over section properties as:

$$EA = \int_A E_t dA = \sum_{i=1}^{nc+ns} E_{ti} A_i \tag{5}$$

$$EM = \int_A E_t y dA = \sum_{i=1}^{nc+ns} E_{ti} y_i A_i \tag{6}$$

$$EI = \int E_t y^2 dA = \sum_{i=1}^{nc+ns} E_{ti} (y_i^2 A_i + I_i) \tag{7}$$

in which E_{ti} is the tangent modulus at the center of a finite area A_i of the layer at depth y_i from the centroid of the uncracked transformed section. E_{ti} and A_i may belong to one of the *ns* reinforcement layers or one of the *nc* concrete layers composing the section. I_i is the moment of inertia of the concrete layer about its local centroid. Inclusion of the last term in Eq. (7) increases accuracy and would yield exact results if E_t were constant. The accuracy of Eqs. (5) through (7) depends on the number of layers and the state of strains over the cross section.

Evaluating the force vector in Eq. (4) requires computing the axial force, *N*, and moment, *M*, over the cross section by summing them over the total number of layers.

$$N = \int_A \sigma dA = \sum_{i=1}^{nc+ns} \sigma_i A_i \tag{8}$$

$$M = \int_A \sigma y dA = \sum_{i=1}^{nc+ns} \sigma_i y_i A_i \tag{9}$$

3. Improved variable layering system

This method is based on implicitly dividing the concrete cross section into a few layers, each of which is under a continuous state of stress and tangent modulus. The number and size of layers are not predefined but rather depend on the state of strain, the stress-strain relationship and the shape of the section. Gaussian numerical integration is performed over each layer to evaluate its contribution to the total forces or stiffness of the section under consideration.

3.1. Defining a typical concrete layer

A critical zone is defined as the area in the section bounded by two discontinuities in concrete property curves or a geometric discontinuity in the width of the section. Prior to defining a layer, the strains at the top and bottom edges of the cross section under consideration should be determined. In the finite element analysis, this is attained using the strain-displacement relationship, which may be expressed as:

$$\varepsilon(x, y)=\{B_s\}\{d\}+1/2\{d\}^T\{B_L\}\{d\} \tag{10}$$

Substituting the appropriate x and y values in the above equations gives ε_t and ε_b, where the former is the strain at the top of the section while the latter is the strain at the bottom.

The procedure for determining a typical layer J can be illustrated with reference to Fig. 1(a) in which a strain distribution due to loading Q is assumed. The top strain under this loading stages is termed ε_{t_Q}, while the strain at the bottom is termed ε_{b_Q}. Now, consider that ε_{c1} and ε_{c2} are two consecutive critical strains among a set of predefined critical strains as will be illustrated later. Following the assumption of linear strain distribution over the cross section of depth H, one may obtain the corresponding critical depths that identify the location and height of each individual layer as given by the following equations.

$$\eta_{c1}=\frac{\varepsilon_t-\varepsilon_{c1}}{\varepsilon_t-\varepsilon_b}H \tag{11}$$

$$\eta_{c2}=\frac{\varepsilon_t-\varepsilon_{c2}}{\varepsilon_t-\varepsilon_b}H \tag{12}$$

The term Q is dropped in the above equations for generalization. The height of the layer J that has a strain such that $\varepsilon_{c1}\le\varepsilon\le\varepsilon_{c2}$ is defined by $\Gamma_J=\eta_{c2}-\eta_{c1}$ as shown in Fig. 1(a). Under the subsequent loading condition $Q+\Delta Q$, the top and bottom strains are defined by $\varepsilon_{t\_Q+\Delta Q}$ and $\varepsilon_{b\_Q+\Delta Q}$, respectively as shown in Fig. 1(b). Following the same procedure in defining the location and height of the individual layer characterized by $\varepsilon_{c1}\le\varepsilon\le\varepsilon_{c2}$, it is evident that the height and location of the individual layer under loading $Q+\Delta Q$ would be different from those at loading Q. In general, the characteristics of any layer may change at any subsequent solution increment at which the edge strains are different.

When a discontinuity is encountered within the territory of a layer, as presented in Fig. 2, it is appropriate to split that layer in order to enhance computational accuracy. The figure shows layer J where part of it is located in the web and the other part in the flange. This layer is conveniently divided into two layers: layer J-A in the flange, and layer J-B in the web. In other words, when a

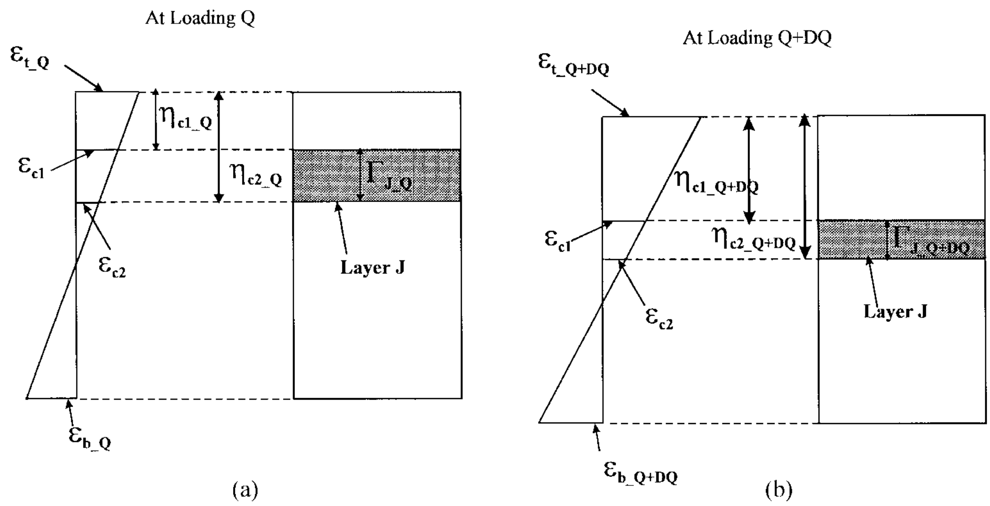

Fig. 1 Defining a typical layer in a rectangular section: (a) layer *J* at loading *Q*; (b) layer *J* at loading *Q*+*DQ*

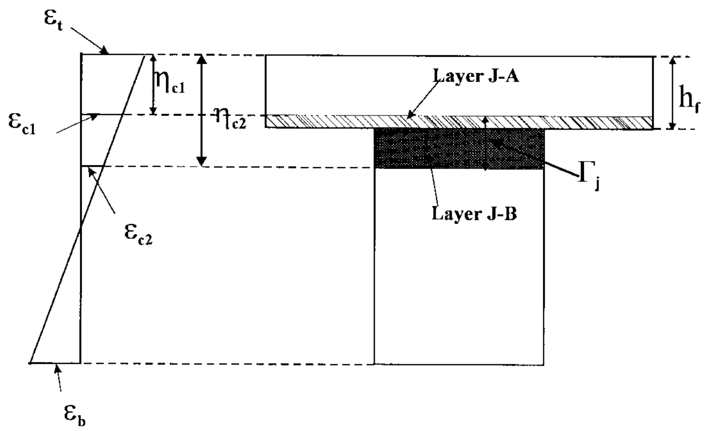

Fig. 2 Defining a layer at discontinuity in a flanged section

discontinuity exists such that $\eta_{c1} < h_f < \eta_{c2}$, it needs to be split into two layers having heights of $\eta_{c2} - h_f$ and $h_f - \eta_{c1}$, respectively.

3.2. Determining the number and depths of layers in a section

The number of concrete layers in a RC section at any loading stage is determined by three factors: the constitutive law of concrete; the loading stage; and the shape of the cross section. For concrete under monotonic uniaxial loading, one can observe some general characteristics governing the stress-strain curves regardless of the mathematical formula. For example, concrete behavior under monotonic static compression can be described by ascending and descending branches. In tension, there are three states: an uncracked state, a tension-stiffening state that is normally modeled by a descending branch, and a fully cracked state. For simplicity, there is no attempts here to make a distinction in the post cracking stage between tension-stiffening and tension-softening states

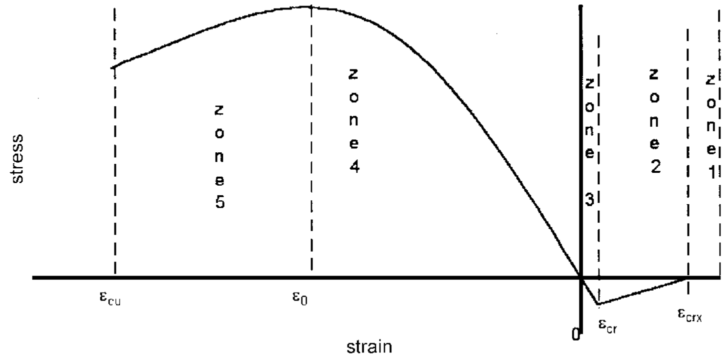

Fig. 3 Major zones in a typical concrete stress-strain relationship

despite the fact the two phenomena are quite different (Barzegar 1989, Cedolin *et al.* 1982). Therefore, a section may be subdivided based on the state of strains into the following zones as illustrated in Fig. 3:

1) The compression zone of post-maximum stress ($\varepsilon \le \varepsilon_0$) (Zone 5 in Fig. 3). This zone represents the descending branch of concrete in compression beyond the strain, ε_0, at maximum stress. Regardless of the actual stress-strain curve, it is customary to model this part by a continuous function, the tangent modulus of which is negative or zero. This zone may or may not exist, depending on the maximum effective strain in compression at that stage of analysis.

2) The compression zone prior to maximum stress ($\varepsilon_0 < \varepsilon \le 0$) (Zone 4 in Fig. 3). This is the zone of the ascending branch in compression, which is marked by a softening and decreasing tangent modulus. Different relationships are described in the literature, but all of them are continuous. With the exception of rare cases in which all of a section is under tension, this layer is more likely to be present, though it could be at the top or bottom of the section.

3) The tension zone prior to cracking. ($0 < \varepsilon \le \varepsilon_{cr}$) (Zone 3 in Fig. 3).

4) The tension zone beyond cracking (tension stiffening zone), which is represented by a descending branch. ($\varepsilon_{cr} < \varepsilon \le \varepsilon_{crx}$) (Zone 2 in Fig. 3). Despite the fact that this zone may or may not contain reinforcements, it is common to represent this zone by an appropriate descending branch with no distinction between the two cases. However, one elegant approach to make a distinction is to model the tension-softening by a suitable descending curve and account for the effect of concrete around the rebars by modifying the rebars properties as proposed by Gilbert and Warner (1978). The former approach was assumed in this study.

5) The zone beyond cracking, where the stress is assumed to be zero (Zone 1 in Fig. 3).

In the current formulation, the maximum number of critical strains, n_1, to define the aforementioned concrete stress-strain curve under elastic nonlinear analysis may be represented by Eq. (13).

$$\{\varepsilon\} = \begin{Bmatrix} \varepsilon_0 \\ 0 \\ \varepsilon_{cr} \\ \varepsilon_{crx} \end{Bmatrix} \tag{13}$$

These strains allow determining the maximum number of layers in the concrete cross section. However, it is obvious that some of the terms in Eq. (13) may become irrelevant for determining the instantaneous layers in a section at an intermediate step in the loading history. Consider, for instance, an uncracked section where compressive strain is below ε_0. From Fig. 3, it is evident that under the above assumption, zones five, two and one are irrelevant. Hence, for this example, the term zero is the active critical strain and it is sufficient to determine the required number of layers in the section as will become obvious later. In general, the active number of critical strains for a particular level of loading may vary depending on the strain variation at moment, *t*, in the solution history.

Therefore, to automate the process of determining the layers at time *t* in the solution history, we need to define a set of instantaneous active critical strains whenever a computation over a cross section is sought. This will be accomplished by ensuring that any term in Eq. (13) that does not satisfy the condition imposed by Eq. (14) be excluded temporarily from the list of critical sections. This action has the effect of specifying a lesser number of concrete layers at time *t*. Therefore, prior to conducting computations on the section, the vector of strains $\{\varepsilon\}$ should be examined to temporarily remove any strain that does not satisfy the following condition:

$$\min\{\varepsilon_t,\ \varepsilon_b\} < \varepsilon_i < \max\{\varepsilon_t,\ \varepsilon_b\} \tag{14}$$

Where ε_t is the strain at the top of the section at time *t*, and ε_b is the strain at the bottom of the section at the same instance. Moreover, ε_i represents the terms in Eq. (13) in which some of them will be outside the section as illustrated by the forgoing example. The elimination process of the terms in Eq. (13) based on condition stated by Eq. (14) yields a vector of active critical strains $\{\varepsilon\}$ having only n_2 active terms for that section at that instance, such that:

$$0 \le n2 \le n1 \tag{15}$$

Once the set of the instantaneous active critical strains is determined as aforementioned, the next step is to determine the locations of the active critical strains over the section in order to determine the boundaries of the active variable layers at time *t* in the solution history. The depth at which an active critical strain is located over the cross section under consideration can be conveniently computed by Eq. (11) after substituting the relevant active critical strain for ε_{c1}. Accordingly, for the set of the active critical strains, there exist corresponding $n2$ active critical depths that can be evaluated by Eq. (11) and written in a vector form as

$$\{\eta\} = \begin{Bmatrix} \eta_1 \\ \eta_2 \\ \cdots \\ \eta_{n2} \end{Bmatrix} \tag{16}$$

In addition to the strain variations caused by the loading level and the general assumptions about the stress-strain relationship based on which Eq. (16) was assembled, the effect of cross section shape needs to be introduced here. The number of instantaneous active concrete layers will be established after combining the section geometry vector $\{g_s\}$, Eqs. (17) or (18) depending on the section type, with the strain depth vector $\{\eta\}$ given by Eq. (16).

For a rectangular section, $\{g_s\}$ contains the following two terms expressed by Eq. (17):

$$\{g_s\} = \begin{Bmatrix} 0 \\ H \end{Bmatrix} \tag{17}$$

Where, H is the total depth of the cross section. To illustrate the role of $\{g_s\}$, consider again the aforementioned uncracked section where compressive strain is below ε_0. It has been shown that for such a section, there is only one active critical strain from Eq. (13), namely, zero. From Eq. (16), there will be only one term η_1. Consequently, the section has two layers: the thickness of the first layer is η_1 while the thickness of the second layer is H-η_1.

On the other hand, for a T-section, the vector contains three essential terms as expressed by Eq. (18).

$$\{g_s\}=\begin{Bmatrix} 0 \\ h_f \\ H \end{Bmatrix} \tag{18}$$

Where, h_f is the depth of the flange.

As a result, the vector of instantaneous critical depths $\{\gamma\}$, which has n_3 terms (n_3=n_2+the number of elements in $\{g_s\}$), at a particular stage is assembled from $\{g_s\}$ and $\{\eta\}$. For a systematic handling of the computations, the n_3 elements of the $\{\gamma\}$ vector should be interspersed by sorting the depth terms in ascending order measured from the top of the section. It may take the form expressed by Eq. (19) where the first term is always zero and the last term is H.

$$\{\gamma\}=\begin{Bmatrix} 0 \\ \eta_1 \\ h_f \\ \cdots \\ \eta_{n3\text{-}1} \\ H \end{Bmatrix} \tag{19}$$

From the vector $\{\gamma\}$, there will be lc active concrete layers at time t, where lc=n3–1; the height of the Jth layer is determined by:

$$\Gamma_J=\gamma_{i+1}-\gamma_i \tag{20}$$

Where J=1,…, lc and i=1, …, lc

3.3. Integration points in a concrete layer

The most accurate of the quadrature formulas in common usage is that of Gauss which involves unequally spaced points that are symmetrically placed (Weaver *et al.* 1984). The procedure for Gauss's method is expressed in a dimensionless coordinate system with its origin at the center of the range of integration. It is assumed here that a three-point Gaussian integration should give sufficient accuracy for the forces and stiffness parameters of a typical region. The range of the integration is usually taken from −1 to +1 and the integration points are located at $-\sqrt{3/5}$, 0, $\sqrt{3/5}$. When the locations of these points are expressed in terms of the height Γ_J, they correspond to the following vector:

$$\begin{Bmatrix} \frac{1}{2}\left(1-\sqrt{\frac{3}{5}}\right) \\ 1/2 \\ \frac{1}{2}\left(1+\sqrt{\frac{3}{5}}\right) \end{Bmatrix} \Gamma_j \tag{21}$$

The integration points in a typical layer are shown in Fig. 4. The depth of a typical point measured from the top fiber of the section is obtained by summing the heights of the upper layers and adding the depths given in Eq. (21). For instance, the depth of the first point in a layer is given by Eq. (22).

$$\chi_{1j}=\sum^{j-1} \Gamma_i+\frac{1}{2}\left(1-\sqrt{\frac{3}{5}}\right)\Gamma_j \tag{22}$$

The first term in Eq. (22) should be zero when the locations of the integration points for the first layer are calculated. After the locations of the critical points are defined, the concrete strain at each point can be computed. The flexural strain at any integration point at depth χ_{iJ}, is to be evaluated by Eq. (23), assuming linear strain distribution, or equivalently, using Eq. (10) in a general nonlinear analysis

$$\varepsilon(\chi_{iJ})=\varepsilon_t-\frac{\chi_{iJ}}{H}(\varepsilon_t-\varepsilon_b), \ i=1,2,3 \qquad J=1,2,\ldots, lc \tag{23}$$

3.4. Sectional forces

For each strain computed at an integration point, the corresponding stress will be obtained from the governing stress-strain constitutive relationships. From the computed stresses, the axial force over a layer is given by Eq. (24) while the moment of that layer is computed by Eq. (25). The normal force on the *J*th typical layer is computed from the forces at the three points using Gauss's weighting factors as expressed by the following equation:

$$N_J=\frac{Ac_J}{2}\left[\frac{5}{9}\sigma_{1J}+\frac{8}{9}\sigma_{2J}+\frac{5}{9}\sigma_{3J}\right] \tag{24}$$

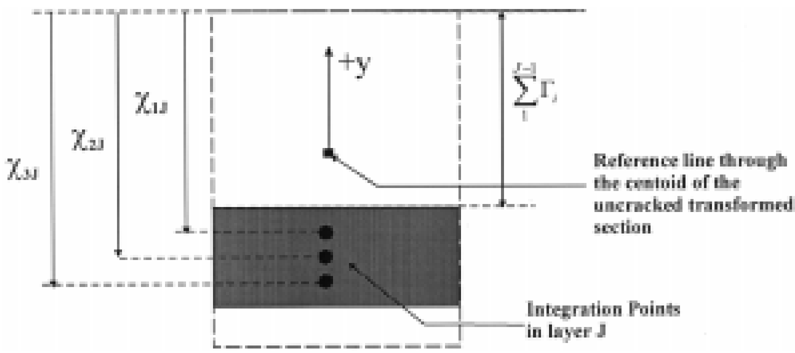

Fig. 4 Depths of integration points measured from the top fiber of the section for strain computations

where Ac_J is the area, and $\sigma_J's$ are the normal stress at the three integration points in the Jth layer. In a similar manner, the bending moment of a typical layer is computed using the weighting factors by the following equation:

$$M_J = \frac{Ac_J}{2}\left[\frac{5}{9}\sigma_{1J}y_{1J} + \frac{8}{9}\sigma_{2J}y_{2J} + \frac{5}{9}\sigma_{3J}y_{3J}\right] \tag{25}$$

where y_{1J}, y_{2J}, and y_{3J} are the depths of the points measured from the reference line which is the centroid of the transformed uncracked section as shown in Fig. 5 and given by the following expression: $y_{iJ} = Z_0 - \chi_{iJ}$ i=1, 2, 3 and J=1, …, lc

The total forces on the section are calculated by summing the contribution of all active concrete layers, lc, and then including the contribution of the reinforcing steel. Because there is no strain variation over a steel layer, the contribution of steel reinforcement to forces and moments will be added in a direct summation to the concrete's contribution as in Eqs. (26) and (27).

$$N = \sum_{j=1}^{j=lc} N_j + \sum_{i=1}^{i=ns} f_{si}A_{si} \tag{26}$$

$$M = \sum_{j=1}^{j=lc} M_j + \sum_{i=1}^{i=ns} f_{si}A_{si}y_{si} \tag{27}$$

where lc is the number of active concrete layers and for a rectangular section has a value ranging between one and five, depending on the state of strain. The situation with the highest number of layers will arise when the section is highly loaded in the inelastic range. The number of reinforcing steel layers in the section is represented by ns. The quantities f_{si}, A_{si}, y_{si} are the stress, area, and moment arm, respectively, of the ith reinforcing steel layer.

3.5. Sectional stiffness parameters

The three section parameters of stiffness, EI, EA, EM have to be evaluated at the onset of every new load increment. First, the strain at each integration point is calculated from Eq. (10). Next, for each strain computed at an integration point, the corresponding tangent modulus is obtained from the appropriate tangent modulus-strain relationship for concrete. Having the required data, one may evaluate the three parameters as described by Eqs. (28) to (30).

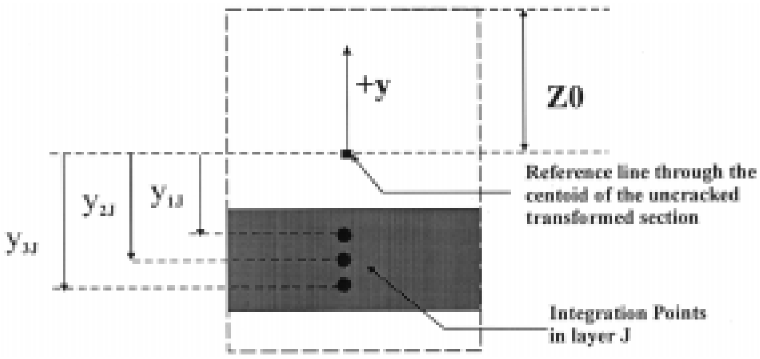

Fig. 5 Depths of integration points measured from the centroid of the section for force and stiffness computations

$$EA_J = \frac{Ac_J}{2}\left[\frac{5}{9}E_{t1J} + \frac{8}{9}E_{t2J} + \frac{5}{9}E_{t3J}\right] \tag{28}$$

$$EM_J = \frac{Ac_J}{2}\left[\frac{5}{9}E_{t1J}y_{1J} + \frac{8}{9}E_{t2J}y_{2J} + \frac{5}{9}E_{t3J}y_{3J}\right] \tag{29}$$

$$EI_J = \frac{Ac_J}{2}\left[\frac{5}{9}E_{t1J}y_{1J}^2 + \frac{8}{9}E_{t2J}y_{2J}^2 + \frac{5}{9}E_{t3J}y_{3J}^2\right] \tag{30}$$

where E_{tJ}'s and y_J's are the tangent moduli of concrete and their corresponding depths at the three integration points in the *J*th layer and A_{cJ} is the area of the layer. The contribution of other layers and reinforcing bars will be added in order to obtain the three parameters as illustrated by the following equations:

$$EA = \sum_{j=1}^{j=lc} EA_j + \sum_{i=1}^{i=ns} E_{si}A_{si} \tag{31}$$

$$EM = \sum_{j=1}^{j=lc} EM_j + \sum_{i=1}^{i=ns} E_{si}A_{si}y_{si} \tag{32}$$

$$EI = \sum_{j=1}^{j=lc} EI_j + \sum_{i=1}^{i=ns} E_{si}A_{si}y_{si}^2 \tag{33}$$

The formulation given above reflects the changes required converting the conventional layered approach to the variable layering system. Accordingly, the RC frame computer program (FRAME-CL) developed previously by the author (Shuraim 1997) was modified to incorporate the improved layering system instead of the conventional layered approach. Fig. 6 shows the outline of the modified program (FRAME-IL) to allow for including the proposed procedure.

4. Results

Two demonstrative examples are given here to allow in-depth understanding of both methods with respect to accuracy, numeric stability, required number of conventional layers, and computational time. The first example uses the two versions of SECTION computer program to assess the two approaches regarding the accuracy of the solution and the required number of conventional layers. The second example uses the two versions of FRAME computer program in order to assess the speed of the two methods.

4.1. Numerical accuracy and stability via an example

First, as shown in Fig. 7, a singly reinforced section was investigated with SECTION-CL and SECTION-IL computer programs. The axial load and bending moment for chosen cases were computed to examine the effect of the number of concrete layers on the resulting forces. Material curves for concrete were as shown in Fig. 3, while rebars were placed in a single layer and were assumed to have an elastic-perfectly-plastic curve. Sectional forces were obtained using these particular concrete layers: 5, 10, 15, 20, 25, 30, 50, 100, and 199 for three selected neutral axis

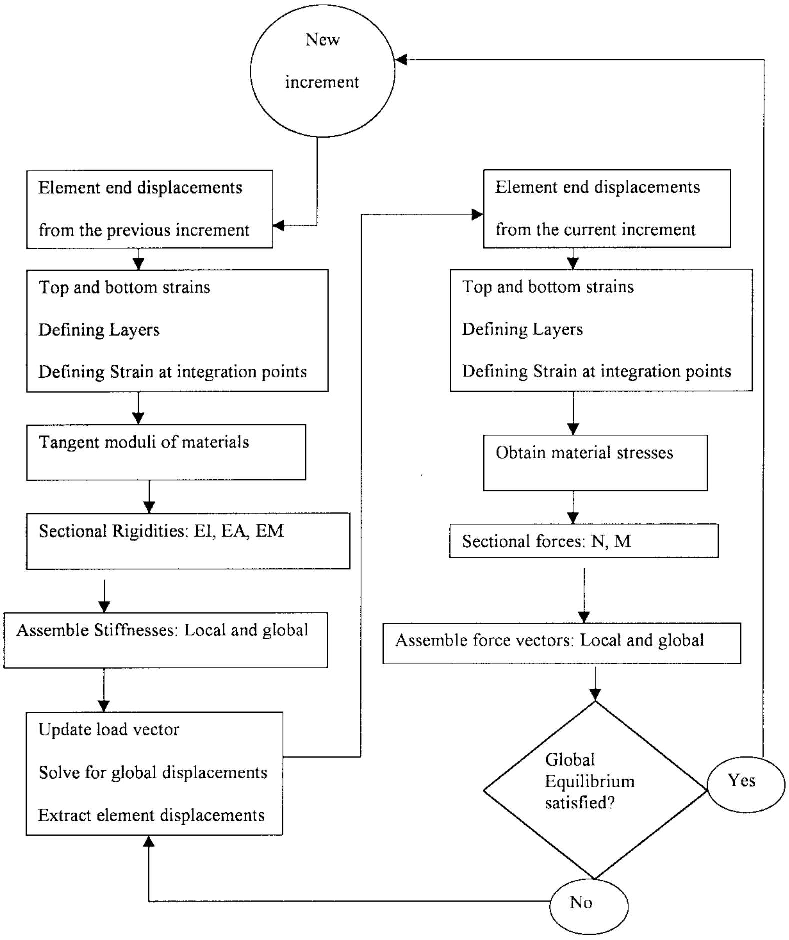

Fig. 6 Outline for the general procedure of the model

depths c=150, 100, and 60 mm, which amount to 0.3H, 0.2H and 0.12 H respectively. In all these cases, the top strain was taken as 0.003 in compression.

The comparison of the two approaches in computing the moment to axial force ratio (eccentricity) is presented in Fig. 7 for two neutral axis depths. For the neutral axis depth of 0.2H, the conventional layered approach shows the eccentricity increasing slightly with the increase in the number of layers until the number becomes twenty, at which point the ratio becomes constant despite any increase in number of layers thereafter. In contrast, the improved layering gives an eccentricity that coincides with eccentricity obtained using of the highest number of layers as shown in the figure. Moreover, for the neutral axis depth of 0.12H, the conventional layered approach shows the eccentricity fluctuating until the number of layers becomes around forty. In contrast, the improved layering gives an eccentricity that coincides with eccentricity obtained using of the highest number of layers as shown in the figure.

The following observations may be made about the conventional layering system based on the case study: (1) the number of layers needed to give an acceptable level of accuracy depends on the neutral axis depth where the higher the neutral axis depth the fewer the layers required and vice

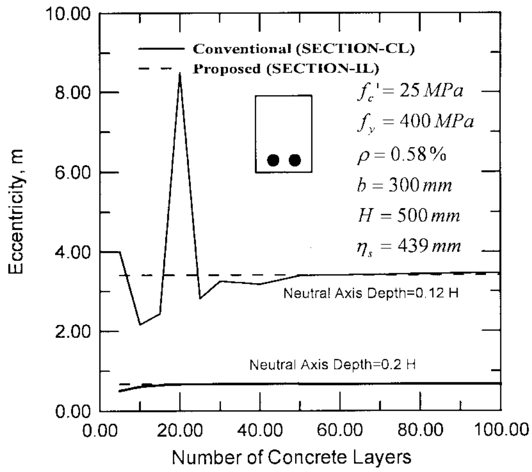

Fig. 7 Eccentricity versus concrete layers for a reinforced concrete section

versa; (2) for the case of low neutral axis depth, the resulting curve in Fig. 7 indicates that numerical instability may arise in the case of insufficient number of layers; (3) different answers may result from differing numbers of layers; (4) a large number of layers are needed to get reasonably accurate results, and consequently requires more computational time.

4.2. Time requirement of the two methods via an example

To get a reasonably good estimate of the computational time consumed by the two methods, the following frame was selected for the analysis. Geometry and general layout are shown in Fig. 8. The same cross section and reinforcement were used for both beams and columns. A set of lateral loads designated by P1, P2, P3 with a relative ratio of 10 : 8 : 7 were applied in addition to the self-weight of the members. Thirty layers were used to represent the section for the conventional layered approach.

As shown in Fig. 9, both methods gave almost identical load-deflection curves. There was a real difference, however, in the computational time required by each method. Fig. 10 shows the time versus incremental load P1. The figure also shows that a large part of the time is consumed at the later stages of the incremental load.

The results indicate that in this example using the improved layering system gives a 62.8% saving in computational time. This substantial saving while maintaining the flexibility and convenience of the conventional layered approach makes the improved layering system highly recommended for complex problems.

5. Comparison with other studies

Program (FRAME-IL) was verified by comparing its prediction of a RC frame to the experimental results as well as to other numerical studies from the technical literature. The portal frame, designated B40, was loaded at two points (Ernst *et al.* 1971) as shown in Fig. 11. It was, also, analyzed by other researchers (Kim *et al.* 1993, El-Metwally *et al.* 1989). Due to symmetry, only one half of the

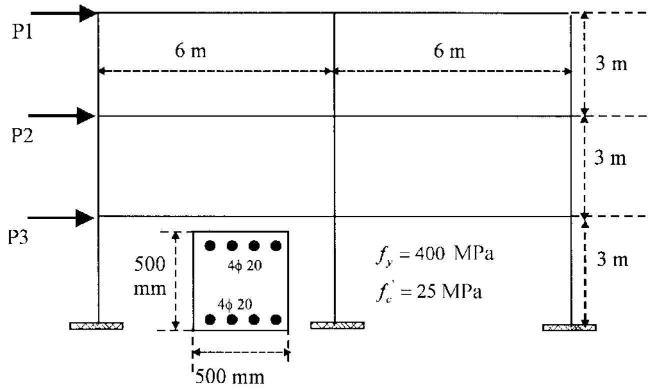

Fig. 8 Material properties and layout for the three-story frame

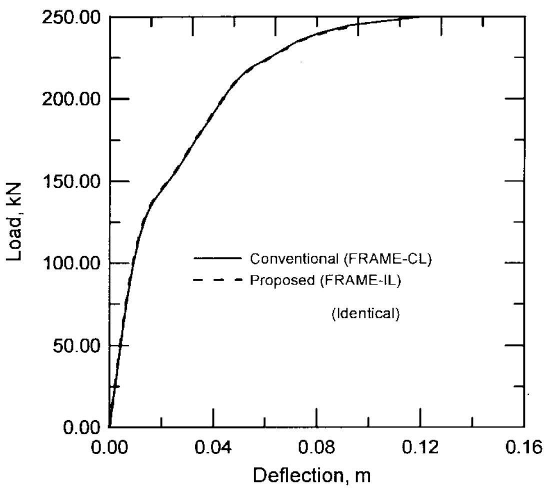

Fig. 9 Load deflection curves for the three-story frame

frame needed to be analyzed. Twelve beam elements were used to model the left half of the frame. The material properties used for the concrete and steel were f_c' =29.1 MPa and f_y=363.9 MPa.

The predicted load-central deflection for the frame is shown in Fig. 12. From the Fig., one may observe that there is agreement with the experimental data for most regions of the load-deflection curve. In particular, there is excellent agreement under service load. Moreover, the program predicted the maximum experimental load with high level of accuracy. The computation time for this problem was 38 seconds on a 486-Dx personal computer.

Also shown in this figure are the results of analytical study proposed by the aforementioned researchers (Kim *et al.* 1993, and El-Metwally *et al.* 1989). It is seen that up to service load, the three curves are in good agreement. For loads higher than service load, Kim's curve shows better agreement with the test. At ultimate load, the current study gives the best prediction; it is followed by the data of Kim *et al.* and to a lesser extent by the data of El-Metwally *et al.* Overall, the proposed numerical solutions were found to be quite rapid and produced an accurate prediction of the test results.

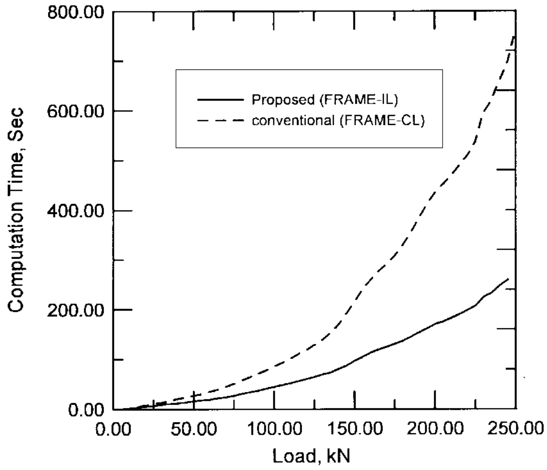

Fig. 10 Time-load curves for the three-story example using both methods

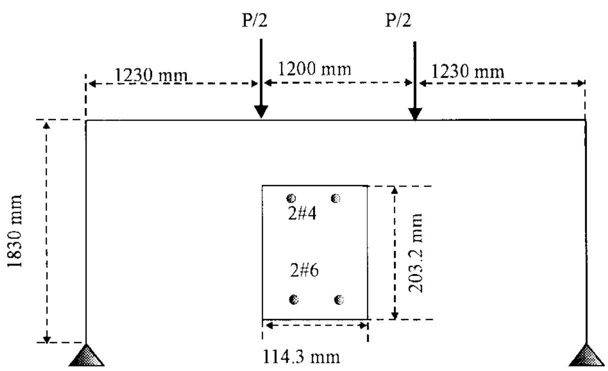

Fig. 11 Loading and geometry of Frame B40

6. Conclusions

In this study, two main tasks were considered: first, the effect of the number of layers on computation accuracy and time requirement was investigated; secondly, a variable layering technique was proposed. Appropriate computer programs were written to fulfil the objectives. Both the proposed and the conventional layered system were examined and compared in order to show the significance of the proposed approach through demonstrative examples. This study indicates that:

1) The number of conventional layers needed to achieve numerical accuracy and stability of a solution is dependent on the state of strain over the section. More layers are needed as the curvature increases.
2) In the proposed method, the layers are defined automatically throughout the analysis history depending on the strain variations, the characteristics of the concrete stress-strain curve and the shape of the cross section.
3) The proposed method can give significant improvement in time requirement and in the solution accuracy in comparison with the conventional layered approach.

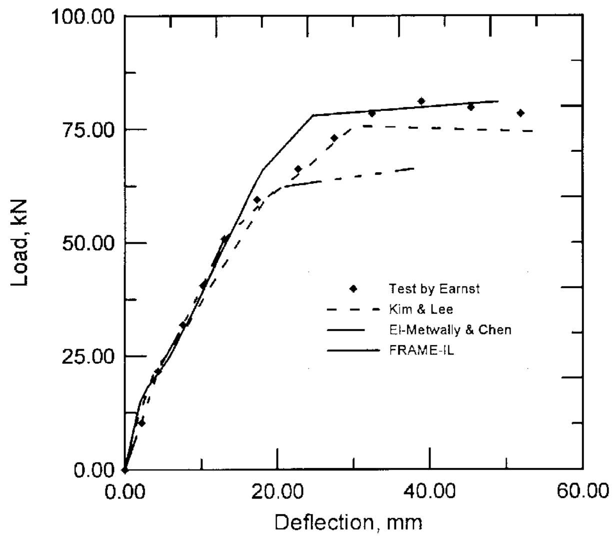

Fig. 12 Load-central deflection curve for Frame B40

References

Abdel Rahman, H.H. and Hinton, E. (1986), “Nonlinear finite element analysis of reinforced concrete stiffened and cellular slabs”, *Comput. Struct.*, **23**, 330-350.

Barzegar, F. (1989), “Analysis of RC membrane elements with anisotropic reinforcement”, *J. Struct. Eng.*, ASCE, **115**, 647-665.

Bazant, P., Pan, J. and Cabot, G.P. (1987), “Softening in reinforced concrete beams and frames”, *J. Struct. Eng.*, ASCE, **113**, 2333-2347.

Bresler, B. and Selna, L.G. (1964), “Analysis of time-dependent behavior of reinforced concrete structures”, *Symposium on Creep of Concrete*, ACI SP-9, 115-127.

Cedolin, L., Darwin, D., Ingraffea, A.R., Pecknold, E.A. and Schnobrich, W.C. (1982), “Concrete cracking,” STATE OF THE ART Report on Finite Element Analysis of Reinforced, ASCE Special Publications, ASCE, New York, 545.

El-Metwally, E. and Chen, W.F. (1989), “Nonlinear behavior of R/C frames”, *Comput. Struct.*, **32**, 1203-1209.

Ernst, C., Smith G.H. and Riveland, A.R. (1971), “Basic reinforced concrete frame performance under vertical and lateral loads”, ACI *J.*, **70**, 261-269.

Gilbert, R.I. (1979), “Time-Dependent analysis of reinforced and prestressed concrete slabs”, *Proceeding of the Third International Conference in Australia on Finite Element Methods*, The University of New South Wales, 215-230.

Gilbert, R.I and Warner, R.F. (1978), “Tension stiffening in reinforced concrete slabs ”, *J. Struct. Div.*, ASCE, **104**, 1885-1900.

Izzuddin, A., Karayannis, C.G. and Elnashai, A.S. (1994), “Advanced nonlinear formulation for reinforced concrete beam-columns,” *J. Struct. Eng.*, ASCE, **120**, 2913-2934.

Kang, Y-J. and Scordelis, A.C. (1980), “Nonlinear analysis of prestressed concrete frames ”, *J. Struct. Div.*, ASCE, **106**, 445-462.

Kim, K. and Lee, T.G. (1992), “Nonlinear analysis of reinforced concrete beams with softening”, *Comput. Struct*, **44**, 567-573.

Kim, K. and Lee, T.G. (1993), “Failure behavior of reinforced concrete frames by the combined layered and nonlayered method”, *Comput. Struct*, **48**, 819-825.

Martin, H.C. (1965), “On the derivation of stiffness matrices for the analysis of large deflection and stability problems”, *Proc. 1st Conf. Matrix Methods Struct. Mech.*, Wright-Paterson AFB, Ohio, AFFDL-TR-66-80, 697-715.

Marzouk, M. and Chen, Z. (1993), “Finite element analysis of high-strength concrete slabs”, ACI *Struct. J.,* **90**, 505-513.

Polak, M.A. and Vecchio, F.J. (1993), “Nonlinear analysis of reinforced -concrete shells”, *J. Struct. Eng.,* ASCE, **119**, 3439-3462.

Selna, L.G. (1969), “Creep, cracking, and shrinkage in concrete framed structures”, *J. Struct. Div.,* ASCE, **95**, 2743-2761.

Shuraim, A.B. (1990), “Slenderness effects in prestressed concrete columns”, Ph.D. Dissertation, The University of Michigan, Michigan.

Shuraim, A.B. (1997), “Lateral stiffness of reinforced concrete frames.” *Comput. Struct*., **64**, 771-782.

Sun, C.H., Bradford, M.A. and Gilbert, R.I. (1993), “Nonlinear analysis for concrete frame structures using the finite element method”, *Comput. Struct*, **48**, 73-79.

Weaver, W. and Johnston, P.R. (1984), *Finite Element for Structural Analysis*, Prentice-Hall, Inc, 403.

Notation

$[k_m]$	: material tangent stiffness matrix of a typical beam-column element
$\{B\},\{B_l\},\{B_s\}$	: total, nonlinear and linear strain-displacement vectors
$\{d\},\{r\}$	: displacements and internal forces at the end of a typical beam-column element
$\{g_s\}$	: depths of critical boundaries of a section
$\{\eta\}$	: depths that define layer boundaries based on active critical strains
$\{\varepsilon\}$	: a set of critical concrete strains
$\{\gamma\}$	: total critical depths in a section
A, Ac	area of a section or a layer
b, H, h_f	: width, total height, and flange height of the section
EA, EI, EM	: the axial, flexural, and the coupling axial-rotational rigidities
l	: the length of a typical beam-column element;
x, y	: Cartesian coordinates with origin at the center of the initial transformed section;
I	: moment of inertia
E_t	: tangent modulus
f_c', f_y	: concrete compressive strength and yield strength of reinforcing steel
M, N	: bending moment and normal force
Q	: applied load
u, v	: linear longitudinal and cubic transverse displacement fields
nc, lc	: number of concrete conventional and variable layers
$n1$, $n2$, $n3$	: number of critical depths
n_s	: number of reinforcement layers
Γ	: height of a layer
χ_{iJ}	: depth of ith integration point in the jth layer from the top fiber
y_{iJ}	: depth of ith integration point in the jth layer from the centroid
ε	: strain
r	: reinforcement ratio
s	: normal stress
ε_{cr}, ε_{crx}, ε_0, ε_{cu}	: strains defined in Fig. 2
ε_t, ε_b	: top and bottom strains in a section
Z_0	: the depth of the section centroid assuming transformed uncracked section as shown in Fig. 5